



Hedgehog signaling is necessary and sufficient to mediate craniofacial plasticity in teleosts

Dina Navon^a, Ira Male^b, Emily R. Tetrault^b, Benjamin Aaronson^c, Rolf O. Karlstrom^c, and R. Craig Albertson^{c,1}

^aGraduate Program in Organismal and Evolutionary Biology, University of Massachusetts, Amherst, MA 01003; ^bGraduate Program in Molecular and Cellular Biology, University of Massachusetts, Amherst, MA 01003; and ^cDepartment of Biology, University of Massachusetts, Amherst, MA 01003

Edited by Clifford J. Tabin, Harvard Medical School, Boston, MA, and approved June 4, 2020 (received for review December 12, 2019)

Phenotypic plasticity, the ability of a single genotype to produce multiple phenotypes under different environmental conditions, is critical for the origins and maintenance of biodiversity; however, the genetic mechanisms underlying plasticity as well as how variation in those mechanisms can drive evolutionary change remain poorly understood. Here, we examine the cichlid feeding apparatus, an icon of both prodigious evolutionary divergence and adaptive phenotypic plasticity. We first provide a tissue-level mechanism for plasticity in craniofacial shape by measuring rates of bone deposition within functionally salient elements of the feeding apparatus in fishes forced to employ alternate foraging modes. We show that levels and patterns of phenotypic plasticity are distinct among closely related cichlid species, underscoring the evolutionary potential of this trait. Next, we demonstrate that hedgehog (Hh) signaling, which has been implicated in the evolutionary divergence of cichlid feeding architecture, is associated with environmentally induced rates of bone deposition. Finally, to demonstrate that Hh levels are the cause of the plastic response and not simply the consequence of producing more bone, we use transgenic zebrafish in which Hh levels could be experimentally manipulated under different foraging conditions. Notably, we find that the ability to modulate bone deposition rates in different environments is dampened when Hh levels are reduced, whereas the sensitivity of bone deposition to different mechanical demands increases with elevated Hh levels. These data advance a mechanistic understanding of phenotypic plasticity in the teleost feeding apparatus and in doing so contribute key insights into the origins of adaptive morphological radiations.

ecodevo | phenotypic plasticity | flexible stem | craniofacial | hedgehog signaling

Phenotypic plasticity is the capacity of a single genotype to produce multiple phenotypes in response to environmental input (1). This ability may increase fitness in novel or fluctuating environments, which suggests that plasticity is adaptive and, therefore, subject to selection itself (2). While sufficient levels of genetic variation have been detected to allow plasticity to respond to selection (3), uncovering its proximate genetic basis has remained a significant challenge especially in vertebrates. While some recent work has begun to delve into this topic by examining differential gene expression across various plastic responses (4–9), much of this research focuses on correlations between gene expression and relevant plastic response. This approach, despite being a powerful demonstration of the genetic factors underlying individual-level plasticity, cannot tease apart whether those molecular differences are the cause or the consequence of these plastic responses, thereby limiting our understanding of how plasticity manifests over the course of development and how it evolves over time.

There is growing evidence in support of the idea that plasticity can bias evolutionary trajectories via the flexible stem hypothesis, which postulates that developmental plasticity in an ancestral population can influence the direction of evolution by exposing novel genetic variation to selection. Under this model, an ancestral population invades a novel habitat and exhibits behavioral plasticity

that leads to subsets of the population exploiting distinct ecological niches, such as different food types. Within a single generation, plasticity in feeding anatomy may lead to more efficient food capture and/or processing in each environment. If beneficial, newly exposed phenotypic variation may be targeted by selection, and if new foraging environments are stable, evolution will favor the canalization of plastic phenotypes through genetic assimilation (10). Implicit to the flexible stem hypothesis is the idea that the same molecular mechanisms underlie both the plasticity and the evolution of key phenotypes (11). In this way, genetic variation in the same pathways that enable plasticity may be selected for and fixed in order to canalize the phenotype (i.e., genetic assimilation, *sensu* Waddington, ref. 10). Support for the flexible stem hypothesis has been documented at the phenotypic level in several important adaptive radiations including Darwin's finches (12), stickleback (13), and cichlids (14); however, we are only just beginning to understand this phenomenon at the genetic level (11).

The cichlid feeding apparatus has long been of interest to biologists owing to its extensive and rapid evolutionary divergence (15) and high degree of phenotypic plasticity (16–18). This combination of morphological diversity and plasticity within a single trait has led to the hypothesis that the cichlid feeding apparatus represents a morphological flexible stem (18). Here, we test this hypothesis by examining the molecular mechanisms that confer environmental sensitivity in the cichlid feeding apparatus focusing on the Hh signaling pathway, which we have

Significance

Phenotypic plasticity has emerged as an important concept in evolutionary biology. It is thought to contribute to an organism's ability to adapt to environmental change within a single generation, which may facilitate survival and increase fitness. Furthermore, plasticity has the potential to bias the direction and/or speed of evolution by changing patterns of phenotypic variation and exposing new genetic variation to selection (i.e., flexible stem evolution). Our understanding of this important phenomenon is incomplete owing to limited knowledge of the molecular underpinnings of reaction norm evolution. Using the teleost feeding apparatus as a model, we explore this open question and show that the Hh signaling pathway underlies the ability of this structure to respond plastically to alternate feeding regimes.

Author contributions: R.O.K. and R.C.A. designed research; D.N., I.M., E.R.T., B.A., and R.C.A. performed research; R.O.K. contributed new reagents/analytic tools; D.N., E.R.T., and R.C.A. analyzed data; and D.N. and R.C.A. wrote the paper.

The authors declare no competing interest.

This article is a PNAS Direct Submission.

This open access article is distributed under [Creative Commons Attribution-NonCommercial-NoDerivatives License 4.0 \(CC BY-NC-ND\)](https://creativecommons.org/licenses/by-nc-nd/4.0/).

Data deposition: All data have been deposited on Dryad (DOI: [10.5061/dryad.jm63xs7jq](https://doi.org/10.5061/dryad.jm63xs7jq)).

¹To whom correspondence may be addressed. Email: albertson@bio.umass.edu.

This article contains supporting information online at <https://www.pnas.org/lookup/suppl/doi:10.1073/pnas.1921856117/-DCSupplemental>.

First published July 27, 2020.

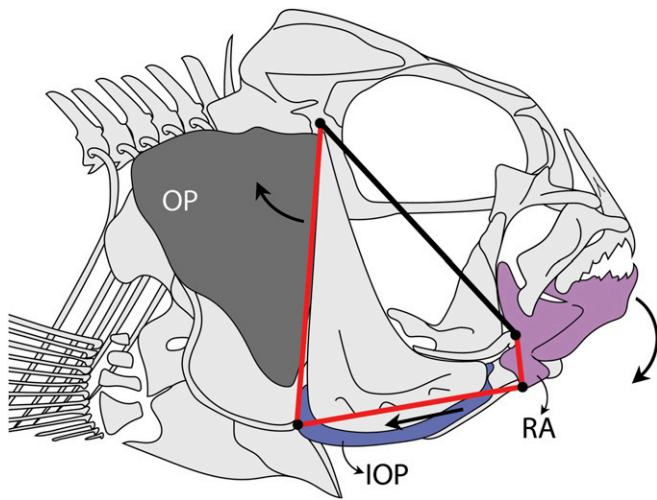


Fig. 1. A four-bar linkage chain is shown describing the kinematics of lower jaw opening in the cichlid skull (29). The three red bars represent movable links, while the single black bar is a fixed link. The system is driven by the levator opercula muscle (not shown), which originates on the skull and inserts along the dorsal aspect of the opercle bone (OP, gray). With the contraction of this muscle, the OP (input link) swings posteriodorsally, pulling the retroarticular process ([RA], output link) of the lower jaw (purple) through the interopercle (IOP) bone (blue, coupler link), which results in lower jaw depression via rotation around the mandible–quadrate joint, located just dorsal to the RA. Variation in the geometry of this linkage will influence the efficiency of the system (e.g., output per unit input) and is associated with cichlid species adapted to different diets (14, 20). Notably, the shapes of 2/3 moveable links (i.e., the IOP and RA links) in this system are associated with and responsive to Hh signaling levels (13, 14).

previously implicated in the evolutionary divergence of cichlid foraging architecture (19, 20).

The Hh pathway is a strong candidate for enabling plasticity in the cichlid jaw, given that it has been implicated in regulating plasticity in both vertebrates and invertebrates (21, 22). It also plays important roles in bone development (23) and is associated with cichlid craniofacial bone formation (19, 20). Furthermore, Hh signaling is inextricably linked to the primary cilium, an important mechanosensor of eukaryotic cells (24). Primary cilia are found on myriad cell types, including bone progenitors (25), and mice lacking primary cilia on bone cells are unable to remodel their bone in response to differential mechanical load (26). Major components of the Hh pathway localize to this organelle, and in the absence of a cilium, a Hh signal cannot be transduced. For these reasons, the primary cilium has been referred to as the “Hh signal transduction machine” (27).

Previous work from our laboratory has implicated *ptch1*, a key component of the Hh pathway, in mediating the evolutionary divergence of bony elements important for feeding kinematics in cichlids (19, 20). In particular, genetic variation at this locus as well as differential expression of *ptch1* messenger RNA (mRNA) were shown to be associated with differences in craniofacial geometry predicted to influence the functional trade-off between speed and power during jaw rotation (Fig. 1). In addition, *ptch1* was shown to be differentially expressed during a plastic response in larval cichlid jaws (28). This finding is similar to other studies that have revealed differential transcript abundance during the plastic response of cichlid pharyngeal jaw morphology (29, 30); however, it remains unclear whether *ptch1*/Hh, or any other differentially expressed transcript, represents a mechanism facilitating plasticity or simply a transcriptional output associated with making more bone.

Distinguishing between these possibilities requires manipulating the pathway under different foraging conditions. Three general outcomes may be expected from such an experiment (Fig. 2). The first represents the null hypothesis (Fig. 2A) where bone growth is not different across genotypes or environments. The second outcome (Fig. 2B) would be expected if Hh signaling regulates bone growth but not plasticity. Here, bone growth may be plastic, but the relative influence of Hh levels on bone deposition will be the same across environments. Alternatively, if Hh signaling influences bone plasticity, the effect of Hh levels on bone growth is expected to be specific to a particular foraging environment such that increased Hh levels will increase the sensitivity of bone to the foraging environment (i.e., steep reaction norm), whereas reduced levels will decrease the sensitivity of bone (i.e., flat reaction norm) (Fig. 2C). Support for the third hypothesis would identify new roles for Hh signaling in bone remodeling and provide new insights into the genetic basis for craniofacial plasticity. Furthermore, based on previously published work on Hh signaling and the evolution of cichlid jaw shape, such data would provide molecular support for the long-held hypothesis that the cichlid feeding apparatus represents a morphological flexible stem (18).

Results and Discussion

Divergent Patterns and Magnitudes of Plasticity among Cichlid Species.

We examined craniofacial plasticity in three cichlid species that vary in terms of their positions along a conserved ecomorphological continuum and exhibit distinct *ptch1* allele frequencies and expression levels (19, 20). The primary axis of morphological variation among cichlid lineages is similar to that of many other teleosts and may be characterized as a continuum between benthic and pelagic foraging species (31). Prey items in the benthos can be tough (e.g., filamentous algae) or hard (e.g., snails) and require power to consume, whereas prey in the pelagic zone tend to be elusive and requires speed to capture. Anatomical configurations of species arrayed along this ecological axis often reflect a functional tradeoff between power and speed. For instance, *Labeotropheus fuelleborni* (LF) are obligate benthic foragers that scrape attached filamentous algae from the substrate using robust and highly specialized foraging structures (30). *Maylandia zebra* (MZ) are true generalist feeders that forage by combing loose algae from rocks as well as by suctioning plankton from the water column (32). They possess longer and more gracile feeding architectures to accommodate these tasks. *Tropheops* sp. red cheek (TRC) feed from the benthos using a

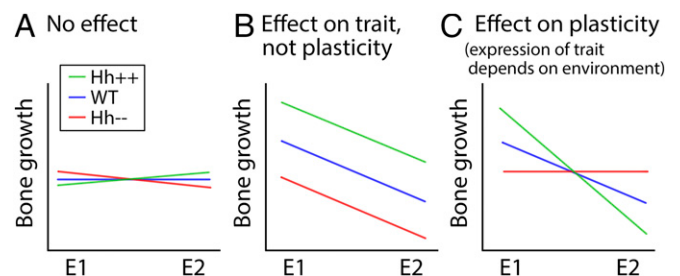


Fig. 2. Predictions are shown for the possible roles of Hh signaling on bone growth and plasticity. The null hypothesis is that bone growth is not plastic, and manipulation of Hh levels has no effect on bone growth (A). Based on previous work from many laboratories, we do not expect this to be the case. Hh signaling is known to play important roles in bone development (15), and the cichlid jaw has been shown to be plastic (27). Another possible outcome is that Hh levels influence bone growth but that the relative effect is similar across environments (B). Finally, we may find that Hh levels influence plasticity such that the effect of Hh levels on bone growth depends on the environment (C). For the experiments in this paper, E1 and E2 represent alternate feeding regimes.

bite-and-twist mode but will also forage on loose material via sifting and suction feeding (32) and exhibit feeding morphologies roughly between those of LF and MZ (33). We predict that the two foraging generalists MZ and TRC will exhibit a measurable plastic response when reared on alternate feeding regimes. Since the ability to mount a plastic response is predicted to come at a cost (3), we predict further that the foraging specialist LF will exhibit a more limited plastic response.

We subjected all three species to alternate foraging treatments in which families were split and reared on diets that mimicked either benthic/biting or pelagic/sucking modes of feeding (34, 35) (Fig. 3A). While the mode of food delivery varied, each treatment involved the same diet to ensure that nutrient content was the same between treatments. Phenotypic response was defined as the rate of bone matrix deposition within several craniofacial bones, assayed by the distance between fluorescent bands that resulted from injecting alizarin red at the beginning and calcein green at the end of each foraging trial (36) (Fig. 3A). We found that MZ and TRC consistently produced a measurable plastic response, but, surprisingly, their reaction norms were in the opposite direction (Fig. 3D–G and L and Table 1). The benthically inclined generalist TRC showed significantly higher rates of bone deposition when reared in the benthic treatment, whereas the more pelagic generalist MZ exhibited higher rates in the pelagic treatment. This difference suggests that the feeding apparatus of TRC is more responsive to benthic foraging, whereas the head skeleton of MZ is more responsive to suction feeding. While unexpected, we posit that this result may be related to species-specific facial geometries and feeding kinematics. MZ possess relatively long horizontally directed jaws that are well designed for suction feeding, an action that involves the rapid opening, protruding, and closing of the jaws. Since suction feeding on small prey will require many foraging strikes to obtain sufficient amounts of food, this action is likely associated with low amplitude but high frequency cyclical loading of the skull. Alternatively, TRC possess short and more ventrally directed jaws, better adapted for a biting mode of feeding, which should result in the production of high amplitude but low frequency static load as more food can be obtained per bite. Thus, the overall load regime for MZ may be higher in the pelagic environment, driven by cyclical load, whereas loads for TRC may be higher in the benthic environment, driven by static load. Finally, we found that the obligate benthic forager LF showed no difference in rates of bone deposition across treatments (Fig. 3L and Table 1), which was consistent with our initial prediction. Patterns and magnitudes of plasticity were highly similar across all bones (Table 1), suggesting a consistent global response to alternate foraging environment in different cichlid species. The observation that closely related species exhibit markedly different magnitudes and directions of plasticity underscores the important link between feeding kinematics and bone remodeling, as well as the evolutionary potential for this trait.

Plastic changes in bone deposition are consistent with previously published reports describing plasticity in bone shape. The relatively short duration of our experiment (~1 mo) was not optimal for documenting global shape changes, which manifest over a period of several months (34, 35); however, differences in the growth of key bony processes as measured by deposition forecast differences in geometry. For instance, we have previously documented plasticity in the relative height of the cichlid lower jaw (i.e., mechanical advantage) in response to the same alternate foraging treatments (35), and this variation in shape is largely driven by differences in the height of the ascending arm of the articular for which we document clear differences in bone deposition rates. These data provide a more comprehensive understanding of how plastic changes in shape are regulated by mechanisms operating at the tissue level.

Ptch1 Expression Is Associated with Rates of Bone Deposition. We next quantified mRNA levels of the Hh transcriptional target *ptch1* in the bones of the species that exhibited craniofacial plasticity. We focused the analysis on the opercle (OP) bone series because of its important role in fish feeding (37), as well as previous data showing that core parts of this complex are responsive to Hh manipulation in cichlids (20). We found that *ptch1* mRNA levels were higher in TRC from the benthic treatment (benthic mean = 0.0058, CI = 0.0035; pelagic mean = 0.0019, CI = 0.0003), whereas *ptch1* expression was higher in MZ from the pelagic treatment (benthic mean = 0.0013, CI = 0.0002; pelagic mean = 0.0031, CI = 0.001) (SI Appendix, Fig. S1). These data are consistent with the phenotypic results presented above and demonstrate a strong positive association between Hh signaling levels and rates of bone deposition, regardless of the specific environmental condition in which the fish were reared. They cannot, however, speak to whether Hh signaling is the cause or the response of craniofacial plasticity. To address this outstanding question, we turned to the zebrafish model where we could directly test gene-by-environmental effects on bone deposition using transgenic systems.

Hh Levels Influence Craniofacial Bone Plasticity. To test the hypothesis that Hh signaling regulates the ability of craniofacial bone to respond plasticity to different foraging regimes, we up- and down-regulated Hh signaling levels in zebrafish using heat-shock-promoter driven transgenes (38). Zebrafish were forced to feed in benthic or pelagic conditions similar to cichlids. Between fluorochrome injections, transgenic fish were heat-shocked for 1.5 h/day to globally activate expression of either *shha* via the transgene *Tg(hsp70l:shha-EGFP)* (where EGFP represents enhanced green fluorescent protein) or a dominant repressor form of the Hh-responsive transcription factor *gli2* via *Tg(hsp70l:gli2DR-EGFP)* (38). We confirmed that the transgenes up- and down-regulated Hh signaling in zebrafish craniofacial bones via qPCR using a panel of four Hh-target genes, *ptch1*, *ptch2*, *hhsp*, and *gli1* (SI Appendix, Fig. S2).

In terms of bone growth, we found that WT zebrafish (i.e., those that were heat-shocked but did not carry the transgene) showed a MZ-like pattern of plasticity with fish from the pelagic treatment depositing more bone than their benthic counterparts (Fig. 3H, I, and M and Table 1). These data matched expectations since zebrafish are pelagic foragers in nature, relying on high frequency cyclical loading of the feeding apparatus, more similar to the pelagic cichlid species, MZ, than the benthic species, TRC. Additionally, we found that down-regulation of Hh signaling resulted in the global reduction (e.g., flattened reaction norms) of craniofacial plasticity across all measured bones (Fig. 3M and Table 1). These results demonstrate that Hh signaling levels are necessary for the craniofacial skeleton to mount a plastic response to alternate foraging behaviors. Notably, experimental up-regulation of Hh signaling resulted in a marked gain of plasticity (e.g., steeper reaction norm) in the interopercle (IOP) (Fig. 3J, K, and M and Table 1), a craniofacial bone that has been shown to be critical for fish feeding (37), sensitive to Hh signaling (20), and responsible for propagating mechanical load to adjacent bones (28) (Fig. 1). These data suggest that mechanical load-induced growth rates in the IOP are Hh dose-dependent. Other craniofacial bones did not respond in the same manner to increased Hh signaling levels with plasticity being either unchanged (e.g., maxilla) or reduced (e.g., OP), which suggests that plasticity in these elements requires endogenous Hh levels, as well as contributions from other molecular mechanisms. Overall, these gain and loss of function data support the hypothesis that Hh signaling levels underlie phenotypic plasticity in key functional components of the craniofacial skeleton (i.e., IOP) in response to different ecologically relevant foraging conditions.

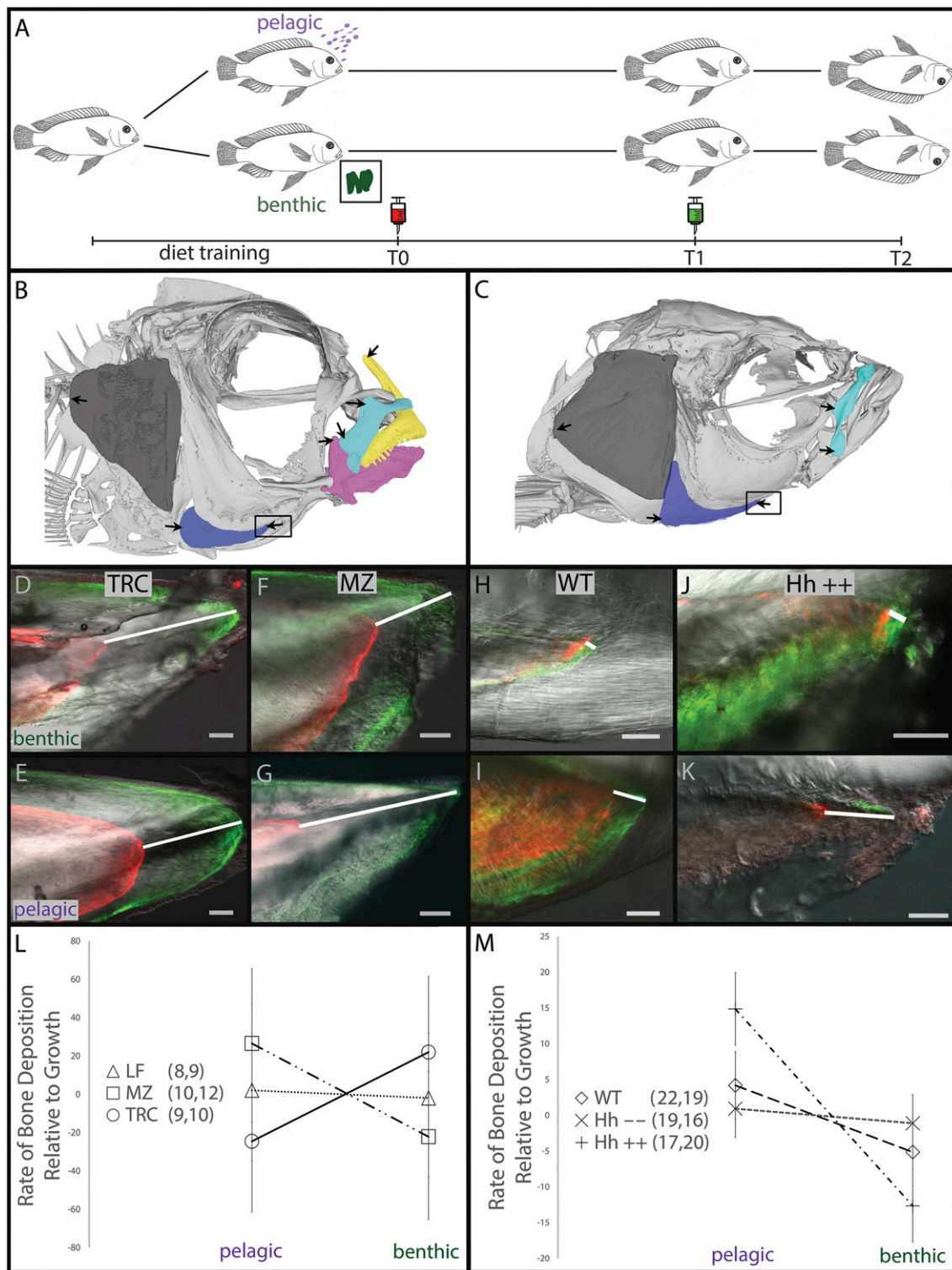


Fig. 3. Rates of bone deposition are shown for different cichlid species and zebrafish genotypes. (A) Schematic of the experimental design: Fish families were split and trained on alternate benthic/pelagic diets for 1 to 2 wk, at time 0 (T0) both groups were injected with a red fluorochrome (alizarin), at T1 (i.e., 1 mo later), a second green fluorochrome (calcein) was injected, and at T2 (i.e., 1 wk later) animals were killed and prepared for bone imaging. (B and C) μ CT reconstructions of a representative cichlid (B) and zebrafish (C) highlighting the bones that were analyzed, including the premaxilla (yellow), maxilla (teal), mandible (pink), IOP (blue), and OP (dark gray). Black arrows in B and C indicate the locations of matrix deposition measurements. Black boxes indicate the anterior portion of the IOP shown in D–K and quantified in L and M. Differences in bone deposition in TRC reared in benthic versus pelagic foraging treatments are illustrated by D and E, respectively. Examples from MZ are shown in F and G, WT zebrafish are shown in H and I, and zebrafish carrying the Hh ++ transgene *Tg(hsp70l:shha-EGFP)* are shown in J and K. White bars indicate the measurement of matrix deposition between T0 and T1. Gray scale bars equal 50 μ m for all panels. (L and M) Reaction norms showing the strength and direction of plasticity in the IOP for the three cichlid species (L) and the three zebrafish genotypes (M). The Hh -- transgene is *Tg(hsp70l:gli2DR-EGFP)*. Symbols represent means. Numbers next to symbols represent sample sizes for each experimental replicate. Error bars are 95% CIs.

Table 1. Mean differences in matrix deposition rates (units = residuals and absolute differences) between treatments are shown for cichlid species and zebrafish genotypes

| Bone | Cichlid species | | | | | | ZF genotype | | | | | |
|----------------------------|-----------------|----------|------------|----------|------------|----------|-------------|----------|------------|----------|------------|----------|
| | LF | | MZ | | TRC | | WT | | Hh -- | | Hh ++ | |
| | Mean diff. | <i>n</i> | Mean diff. | <i>n</i> | Mean diff. | <i>n</i> | Mean diff. | <i>n</i> | Mean diff. | <i>n</i> | Mean diff. | <i>n</i> |
| IOP, post. | 5.25 | 11,11 | 86.41 | 12,11 | 45.83 | 10,10 | 12.28 | 20,22 | 2.40 | 19,19 | 9.75 | 19,19 |
| IOP, ant. | 4.00 | 9,8 | 48.67 | 12,10 | 46.57 | 10,9 | 9.32 | 18,22 | 2.04 | 15,19 | 21.53 | 20,17 |
| Asc. arm of the mandible | 2.54 | 10,11 | 43.54 | 12,10 | 48.22 | 11,9 | — | — | — | — | — | — |
| Maxilla, first wing | 29.27 | 6,8 | 33.32 | 12,9 | 7.86 | 8,8 | 0.99 | 8,7 | 0.14 | 17,13 | 3.43 | 13,7 |
| Maxilla, second wing | 5.80 | 8,11 | 76.92 | 12,8 | 63.69 | 8,10 | 12.04 | 18,23 | 1.15 | 23,20 | 9.71 | 22,18 |
| OP | 21.39 | 10,12 | 130.86 | 12,11 | 89.41 | 9,10 | 31.28 | 24,24 | 18.27 | 23,20 | 4.00 | 27,26 |
| Asc. arm of the premaxilla | 13.78 | 8,10 | 8.80 | 11,11 | 118.64 | 9,8 | — | — | — | — | — | — |

Bone names are listed in the first column, and are color coded following Fig. 3 B and C. Purple colored cells indicate greater deposition, on average, in the pelagic treatment. Purple shading indicates different levels of significance from dark to light: $P < 0.05$, $P \leq 0.1$, $p \sim 0.15$. Green colored cells indicate more deposition in the benthic treatment. Dark green cells indicate significance at $P < 0.05$, and light green cells are significant at $P = 0.06$. Sample sizes for each treatment are also provided as $n = (\text{ben}, \text{pel})$. In zebrafish, a significant treatment-by-genotype effect was detected in the anterior region of the IOP ($F = 3.684$, $P = 0.028$), which is consistent with Hh levels underlying plasticity in this bone. This interaction was approaching significance ($F = 2.732$, $P = 0.069$) for the OP, but this was driven mainly by mean differences being reduced in both *Tg(hsp70l:Gli2DR-EGFP)* (Hh -) and *Tg(hsp70l:shha-EGFP)* (Hh ++) genotypes compared to wild-type (WT) animals.

Conclusions

Identifying the genetic basis of plasticity has broad theoretical implications with respect to the origins of biodiversity. Thirty years ago, Mary Jane West-Eberhard published a seminal review wherein she described how plasticity may accelerate evolutionary processes, including adaptive radiations (39). This framework was subsequently formalized as the flexible stem theory of adaptive radiation (18), which provided a testable hypothesis for how biodiversity may arise in the context of a dynamic ecological landscape, and why evolution sometimes occurs in a predictable manner. For example, why are many of the most extensive adaptive radiations (e.g., anolis lizards, stickleback, and cichlids) characterized by iterative, almost stereotypical, patterns of morphological divergence? The flexible stem hypothesis offers a mechanistic explanation for this observation, which is mainly that genetic variation in the same molecules/pathways that underlie phenotypic plasticity will be targeted by natural selection to drive the evolutionary divergence of key ecological traits. In this way, if the initial plastic response occurs in a predictable direction, then so too should the ultimate evolutionary response through the repeated selection on, and canalization of, cryptic genetic variation that is expressed in novel environments (10, 11, 40–44). Within this framework, our previously published results have established roles for the Hh pathway in the evolution of cichlid feeding morphology, especially for the IOP. This bone plays an important role in feeding behavior (37, 44) and is strongly predictive of ecomorphological divergence (20, 45). Furthermore, experimental manipulation of the IOP has been shown to propagate morphological changes to other craniofacial bones (i.e., the RA) (28), underscoring its critical role in the functional integration of this anatomical complex. In this study, we show that Hh signaling is also both necessary and sufficient to sensitize the IOP to alternate foraging environments. In fact, for the IOP, the foraging environment is a better predictor of bone deposition rates than is the Hh genotype (Fig. 3M). This finding is consistent with a previous genetic mapping study where we showed that genotypic variation at *ptch1* was associated with relative RA length in both benthic/biting and pelagic/suction foraging regimes but that the foraging environment was a better overall predictor of RA length than was the *ptch1* genotype (35).

In general, our work on the association between Hh signaling and bone development suggests greater complexity in the system than has been appreciated. For instance, results presented here complicate the long-held view that Hh signaling is a positive regulator of bone development (44, 46); they show that, for

certain bones, such as the IOP, Hh positively regulates bone deposition in one environment but negatively regulates bone growth in a different environment (Fig. 3M). Thus, it is not simply that increased Hh levels induce bone formation, but rather that Hh signaling helps to sensitize bone cells to receive and/or respond to mechanical input. How this occurs mechanistically will be a topic of future investigation; however, the localization of Hh pathway components to the primary cilium (27), an important mechano-sensitive organelle, may provide a cellular entry point with respect to addressing this question. Our research also highlights a need to better understand the roles for feedback in the system. Specifically, while genes encoding Ptch-membrane receptors are well characterized targets of the Hh signal transduction pathway (38), they also encode proteins that inhibit the system. In the absence of a ligand, Ptch inhibits Smoothen, another receptor, from transducing a signaling into the cell. This makes the observation of greater *ptch1* expression in cichlid species with more robust bone (19, 20) particularly intriguing. Such data could simply be reflective of negative feedback in the pathway (47) whereby a cell makes greater amounts of a receptor molecule to receive high concentrations of ligand, but then these same receptors actively turn the pathway off once ligand molecules are exhausted. Indeed, aberrant activation of Hh signaling in numerous cancers highlights the need for this pathway to be tightly regulated (48). Alternatively, observations in cichlids may point to new roles for the Ptch-dependent, Smo- and Gli-independent, noncanonical Hh pathway in bone development (49). Clearly there is still much to be learned about Hh signaling in bone biology. Regardless of the specific mechanisms at work, the data presented here offer insights into the roles for Hh signaling in bone growth and remodeling. Furthermore, when considered as part of the larger body of literature, they provide robust molecular support for the hypothesis that the cichlid jaw represents a morphological flexible stem (18), thereby advancing our understanding of the origins and diversification of this textbook model of adaptive radiation, as well as our understanding of how phenotypic plasticity acts to shape evolution in general (39).

Materials and Methods

Fish Husbandry. All animals were reared according to protocols approved by the University of Massachusetts Institutional Animal Care and Use Committee (IACUC). Cichlids were raised in 10-gal glass aquaria on standard flake food for 4 mo before families were split into diet treatments and transferred to 40-gal aquaria. For detailed methods on these treatments, see refs. 34 and 35. Briefly, food content and amount was kept consistent across treatments; high-quality algae flaked food (purchased from Worldwide Aquatics, Inc.) was ground and either sprinkled directly into the water column (pelagic

treatment) or mixed with a 1% food-grade agar solution and spread over lava rocks (benthic). Zebrafish were raised in 3-L plastic aquaria on a diet of rotifers from 5- to 12-d postfertilization, and then on a combination of GM-300 (Skretting) and brine shrimp for several months before families were split into diet treatments. All tanks included a mix of transgenic and WT fish; for detailed methods on the generation, validation, and heat-shock protocol of Hh-transgenic zebrafish, see ref. 38. We verified, via qPCR, that heat-shock of these transgenic lines was sufficient to down- and up-regulate Hh transcriptional output in craniofacial bones (i.e., the OP series, see *SI Appendix*, Fig. S2). Pelagic zebrafish received GM-300 sprinkled directly into the water column, while benthic fish received GM-300 mixed with a 1% food-grade agar solution spread over ceramic tiles. Both cichlids and zebrafish were given 1 mo to acclimate to the diet treatments before the start of the experiment; in this time, all benthic fish were feeding readily from rocks or tiles. Each experiment was replicated in two sets of fish; replicate experiments were carried out at different times over the course of a year.

Experimental Design. We quantified rates of bone deposition because this is a likely mechanism through which fish plastically response to alternate foraging environments (36). Fish were anesthetized using MS-222 in cool water during injections and handling. Fish were injected with alizarin red at a concentration of 50-mg fluorochrome/kg fish (T0) and then with calcein green at a concentration of 0.5-mg/kg fish 1 mo later (T1). A week following the final fluorochrome injection, fish were euthanized with a lethal dose of MS-222 (T2). During the time between injections, zebrafish were heat-shocked to 37 °C for 1.5-h daily (38) in their experimental tanks using an automated system adapted from ref. 50. Temperatures were monitored in real time throughout the experiment using an internet-connected Raspberry Pi device. Sacrificed fish were stored in 95% ethanol at 4 °C, which preserved the fluorochrome signal. Fish were weighed before each injection and at the end of the experiment. No statistical differences were noted between any treatment group, which suggests that differential growth was not a confounding factor in our analysis.

Imaging and Quantification of Traits. Craniofacial bones were dissected from the head, cleaned of surrounding soft tissue, flat mounted on glass slides, and imaged with a Zeiss Axioplan2 fluorescent apotome microscope. Bones were imaged in triplicate using a red fluorescent filter, a green fluorescent filter, and a DCIM bright-field view. Cichlid bones were imaged at 10x; zebrafish at 20x. Trunk scales were flat mounted and imaged in the same way. Bone deposition was quantified by calculating the distance between the red and the green fluorochrome labels in each bone using Photoshop.

Statistical Methods. Bone deposition was standardized for individual growth rate using scale growth as the basis for a linear regression (51). Bone deposition data may be found on Dryad (52). All statistical analyses were performed in R (53). Within a genotype or species, Student's *t* tests were performed on the residuals from those regressions in order to determine significant differences in bone deposition between diet treatments. The sample sizes/treatment and *P* values from those *t* tests are reported in Table 1. Reaction norms were generated from those residuals by taking the average bone deposition in a given group and calculating the 95% CI of bone deposition in that group.

qPCR. Quantitative PCR (qPCR) was used to measure the expression of *ptch1* in both TRC and MZ. Primer sequences for cichlid qPCR were as follows: *ptch1* (forward) 5'-TTCTGATGCTGGCCTATGCA-3', *ptch1* (reverse) 5'-CCCCTGAGACTTGGCACAGT-3', β -*actin* (forward) 5'-GTATGTGCAAGCCGGATT-3', and β -*actin* (reverse) 5'-TTCTGACCCATACCCACCAT-3' (19, 28, 54). Zebrafish primers were as follows: *ptch1* (forward) 5'-GCCGCATCCAGGCCAACAT-3', *ptch1* (reverse) 5'-CGTCTCGGAAGCCCGTTGA-3', *ptch2* (forward) 5'-CATCCCATTCAAGGAGAGGA-3', *ptch2* (reverse) 5'-GGCAGGGAATATCAGCAA-3', *hhp1* (forward) 5'-CTGTGGTCTCTCGTGGTAG-3', *hhp1* (reverse) 5'-TTGTGGTCTTTGGGTCCA-3', *gli1* (forward) 5'-GTCATCCGACCTCTCCAAA-3', *gli1* (reverse) 5'-ATGGTGCCACAGACAGATG-3', β -*actin* (forward) 5'-CAACAGGGAAAAGATGACACAGAT-3', and β -*actin* (reverse) 5'-CAGCTGGATGGCAACTG-3' (38). Tissue was taken from the OP series of bones including both the OP and the IOP. RNA was isolated from homogenized tissues using phenol/chloroform extraction and standardized to a common concentration prior to reverse transcription. Finally, levels of gene expression were measured using SYBR Green chemistry (Power SYBR Green Master Mix), and relative quantification (compared to β -*actin*) was analyzed using the comparative CT method (55). All qPCR data may be found on Dryad (52).

Data and Materials Availability. All data are available via Dryad (DOI: [10.5061/dryad.jm63xsj7q](https://doi.org/10.5061/dryad.jm63xsj7q)).

ACKNOWLEDGMENTS. The authors thank past and present members of the R.C.A. laboratory for helpful discussions regarding this project. In addition, we thank R. Shahar and L. Ofer for technical advice on bone deposition experiments, D. Almanzar for building the Raspberry Pi device, and A. J. Conith for the schematic of the cichlid skull in Fig. 1. This work was supported by a Grant from NSF/IOS (1558003) award to R.C.A. and R.O.K.

1. A. D. Bradshaw, Evolutionary significance of phenotypic plasticity in plants. *Adv. Genet.* **13**, 115–155 (1965).
2. C. D. Schlichting, M. Pigliucci, *Phenotypic Evolution. A Reaction Norm Perspective*, (Sinauer Associates, Sunderland, MA, 1998).
3. M. Pigliucci, Evolution of phenotypic plasticity: Where are we going now? *Trends Ecol. Evol.* **20**, 481–486 (2005).
4. L. Luo, Actin cytoskeleton regulation in neuronal morphogenesis and structural plasticity. *Annu. Rev. Cell Dev. Biol.* **18**, 601–635 (2002).
5. M. Flück, H. Hoppeler, "Molecular basis of skeletal muscle plasticity-from gene to form and function" in *Reviews of Physiology, Biochemistry and Pharmacology*, (Springer, Berlin, Germany, 2003), Vol. 146, pp. 159–216.
6. K. M. Baldwin, F. Haddad, Skeletal muscle plasticity: Cellular and molecular responses to altered physical activity paradigms. *Am. J. Phys. Med. Rehabil.* **81** (11, suppl.), S40–S51 (2002).
7. M. Mrdaković et al., Adaptive phenotypic plasticity of gypsy moth digestive enzymes. *Cent. Eur. J. Biol.* **9**, 309–319 (2014).
8. P. Sabat, J. A. Lagos, F. Bozinovic, Test of the adaptive modulation hypothesis in rodents: Dietary flexibility and enzyme plasticity. *Comp. Biochem. Physiol. A Mol. Integr. Physiol.* **123**, 83–87 (1999).
9. F. Gao et al., Phenotypic plasticity of gut structure and function during periods of inactivity in *Apostichopus japonicus*. *Comp. Biochem. Physiol. B Biochem. Mol. Biol.* **150**, 255–262 (2008).
10. C. H. Waddington, Genetic assimilation of an acquired character. *Evol.* **7**, 118–126 (1953).
11. J. M. Gilbert, The flexible stem hypothesis: Evidence from genetic data. *Dev. Genes Evol.* **227**, 297–307 (2017).
12. S. Tebbich, K. Strelny, I. Teschke, The tale of the finch: Adaptive radiation and behavioural flexibility. *Philos. Trans. R. Soc. Lond. B Biol. Sci.* **365**, 1099–1109 (2010).
13. M. A. Wund, J. A. Baker, B. Clancy, J. L. Golub, S. A. Foster, A test of the "flexible stem" model of evolution: Ancestral plasticity, genetic accommodation, and morphological divergence in the threespine stickleback radiation. *Am. Nat.* **172**, 449–462 (2008).
14. M. Muschick, M. Barluenga, W. Salzburger, A. Meyer, Adaptive phenotypic plasticity in the Midas cichlid fish pharyngeal jaw and its relevance in adaptive radiation. *BMC Evol. Biol.* **11**, 116 (2011).

15. G. Fryer, T. D. Iles, *The Cichlid Fishes of the Great Lakes of Africa. Their Biology and Evolution*, (Oliver and Boyd, Edinburgh, 1972).
16. N. Bouton et al., Experimental evidence for adaptive phenotypic plasticity in a rock-dwelling cichlid fish from Lake Victoria. *Biol. J. Linn. Soc. Lond.* **77**, 185–192 (2002).
17. J. R. J. Stauffer, E. van Snik Gray, Phenotypic plasticity: Its role in trophic radiation and explosive speciation in cichlids (Teleostei: Cichlidae). *Anim. Biol.* **54**, 137–158 (2004).
18. M. J. West-Eberhard, *Developmental Plasticity and Evolution*, (Oxford University Press, New York, NY, 2003).
19. R. B. Roberts, Y. Hu, R. C. Albertson, T. D. Kocher, Craniofacial divergence and ongoing adaptation via the hedgehog pathway. *Proc. Natl. Acad. Sci. U.S.A.* **108**, 13194–13199 (2011).
20. Y. Hu, R. C. Albertson, Hedgehog signaling mediates adaptive variation in a dynamic functional system in the cichlid feeding apparatus. *Proc. Natl. Acad. Sci. U.S.A.* **111**, 8530–8534 (2014).
21. T. Kijimoto, A. P. Moczek, Hedgehog signaling enables nutrition-responsive inhibition of an alternative morph in a polyphenic beetle. *Proc. Natl. Acad. Sci. U.S.A.* **113**, 5982–5987 (2016).
22. R. Petrova, A. L. Joyner, Roles for Hedgehog signaling in adult organ homeostasis and repair. *Development* **141**, 3445–3457 (2014).
23. F. Long, Building strong bones: Molecular regulation of the osteoblast lineage. *Nat. Rev. Mol. Cell Biol.* **13**, 27–38 (2012).
24. C. L. Thompson, J. P. Chapple, M. M. Knight, Primary cilia disassembly down-regulates mechanosensitive hedgehog signalling: A feedback mechanism controlling ADAMTS-5 expression in chondrocytes. *Osteoarthritis Cartilage* **22**, 490–498 (2014).
25. J. C. Chen, D. A. Hoey, M. Chua, R. Bellon, C. R. Jacobs, Mechanical signals promote osteogenic fate through a primary cilia-mediated mechanism. *FASEB J.* **30**, 1504–1511 (2016).
26. E. R. Moore, Y. X. Zhu, H. S. Ryu, C. R. Jacobs, Periosteal progenitors contribute to load-induced bone formation in adult mice and require primary cilia to sense mechanical stimulation. *Stem Cell Res. Ther.* **9**, 190 (2018).
27. S. C. Goetz, P. J. Ocbina, K. V. Anderson, The primary cilium as a Hedgehog signal transduction machine. *Methods Cell Biol.* **94**, 199–222 (2009).
28. Y. Hu, R. C. Albertson, Baby fish working out: An epigenetic source of adaptive variation in the cichlid jaw. *Proc. Biol. Sci.* **284**, 1860 (2017).

29. T. Manousaki *et al.*, Parsing parallel evolution: Ecological divergence and differential gene expression in the adaptive radiations of thick-lipped Midas cichlid fishes from Nicaragua. *Mol. Ecol.* **22**, 650–669 (2013).
30. R. F. Schneider, Y. Li, A. Meyer, H. M. Gunter, Regulatory gene networks that shape the development of adaptive phenotypic plasticity in a cichlid fish. *Mol. Ecol.* **23**, 4511–4526 (2014).
31. W. J. Cooper *et al.*, Benthic-pelagic divergence of cichlid feeding architecture was prodigious and consistent during multiple adaptive radiations within African rift-lakes. *PLoS One* **5**, e9551 (2010).
32. A. J. Ribbink *et al.*, A preliminary survey of the cichlid fishes of rocky habitats in Lake Malawi. *S. Afr. J. Zool.* **18**, 149–310 (1983).
33. R. C. Albertson, M. J. Patters, Morphological disparity in ecologically diverse versus constrained lineages of Lake Malawi rock-dwelling cichlids. *Hydrobiologia* **832**, 153–174 (2019).
34. K. J. Parsons, A. Trent Taylor, K. E. Powder, R. C. Albertson, Wnt signalling underlies the evolution of new phenotypes and craniofacial variability in Lake Malawi cichlids. *Nat. Commun.* **5**, 3629 (2014).
35. K. J. Parsons *et al.*, Foraging environment determines the genetic architecture and evolutionary potential of trophic morphology in cichlid fishes. *Mol. Ecol.* **25**, 6012–6023 (2016).
36. A. Atkins, J. Milgram, S. Weiner, R. Shahar, The response of anosteocytic bone to controlled loading. *J. Exp. Biol.* **218**, 3559–3569 (2015).
37. M. W. Westneat, Feeding mechanics of teleost fishes (Labridae; Perciformes): A test of four-bar linkage models. *J. Morphol.* **205**, 269–295 (1990).
38. M. C. Shen *et al.*, Heat-shock-mediated conditional regulation of hedgehog/gli signaling in zebrafish. *Dev. Dyn.* **242**, 539–549 (2013).
39. M. J. West-Eberhard, Phenotypic plasticity and the origins of diversity. *Annu. Rev. Ecol. Syst.* **20**, 249–278 (1989).
40. E. Lafuente, D. Duneau, P. Beldade, Genetic basis of thermal plasticity variation in *Drosophila melanogaster* body size. *PLoS Genet.* **14**, e1007686 (2018).
41. E. Küttner *et al.*, Hidden genetic variation evolves with ecological specialization: The genetic basis of phenotypic plasticity in Arctic charr ecomorphs. *Evol. Dev.* **16**, 247–257 (2014).
42. C. C. Ledón-Rettig, D. W. Pfennig, E. J. Crespi, Diet and hormonal manipulation reveal cryptic genetic variation: Implications for the evolution of novel feeding strategies. *Proc. Biol. Sci.* **277**, 3569–3578 (2010).
43. R. F. Schneider, A. Meyer, How plasticity, genetic assimilation and cryptic genetic variation may contribute to adaptive radiations. *Mol. Ecol.* **26**, 330–350 (2017).
44. G. Lauder, Patterns of evolution in the feeding mechanism of actinopterygian fishes. *Am. Zool.* **22**, 275–285 (1982).
45. P. C. Wainwright, B. A. Richard, Predicting patterns of prey use from morphology of fishes. *Environ. Biol. Fishes* **44**, 97–113 (1995).
46. J. Yang, P. Andre, L. Ye, Y. Z. Yang, The Hedgehog signalling pathway in bone formation. *Int. J. Oral Sci.* **7**, 73–79 (2015).
47. V. Ribes, J. Briscoe, Establishing and interpreting graded sonic hedgehog signaling during vertebrate neural tube patterning: The role of negative feedback. *Cold Spring Harb. Perspect. Biol.* **1**, a002014 (2009).
48. T. K. Rimkus, R. L. Carpenter, S. Qasem, M. Chan, H. W. Lo, Targeting the sonic hedgehog signaling pathway: Review of smoothened and GLI inhibitors. *Cancers (Basel)* **8**, 22 (2016).
49. S. Pietrobono, S. Gagliardi, B. Stecca, Non-canonical hedgehog signaling pathway in cancer: Activation of GLI transcription factors beyond smoothened. *Front. Genet.* **10**, 556 (2019).
50. R. J. Duszynski, J. Topczewski, E. E. LeClair, Simple, economical heat-shock devices for zebrafish housing racks. *Zebrafish* **8**, 211–219 (2011).
51. R. W. Doyle *et al.*, Statistical interrelation of length, growth, and scale circulus spacing: Appraisal of a growth rate estimator for fish. *Can. J. Fish. Aquat. Sci.* **44**, 1520–1528 (1987).
52. C. Albertson *et al.*, Hedgehog signaling is necessary and sufficient to mediate craniofacial plasticity in teleosts. *Dryad*. <https://doi.org/10.5061/dryad.jm63xsj7q>. Deposited 9 July 2020.
53. R Core Team, R: A language and environment for statistical computing. (2017). <https://www.R-project.org/>. Accessed 16 July 2020. (R Foundation for Statistical Computing, Vienna, Austria).
54. K. L. Carleton *et al.*, Visual sensitivities tuned by heterochronic shifts in opsin gene expression. *BMC Biol.* **6**, 22 (2008).
55. K. J. Livak, T. D. Schmittgen, Analysis of relative gene expression data using real-time quantitative PCR and the 2(-Δ Δ C(T)) Method. *Methods* **25**, 402–408 (2001).